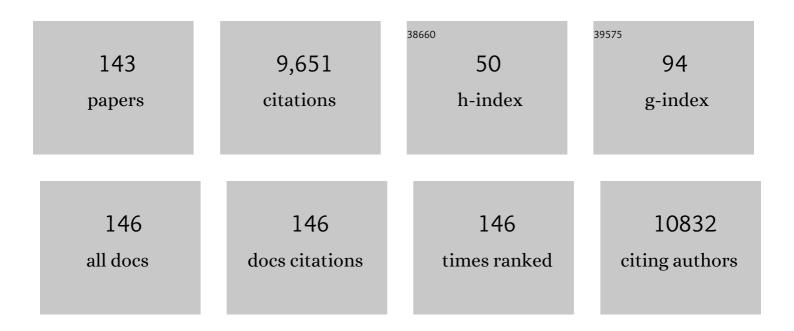


List of Publications by Year in descending order

Source: https://exaly.com/author-pdf/5954957/publications.pdf Version: 2024-02-01



#	Article	IF	CITATIONS
1	A metal–organic framework-derived bifunctional oxygenÂelectrocatalyst. Nature Energy, 2016, 1, .	19.8	1,974
2	Formation of Ni–Fe Mixed Diselenide Nanocages as a Superior Oxygen Evolution Electrocatalyst. Advanced Materials, 2017, 29, 1703870.	11.1	428
3	Flexible all-solid-state hierarchical NiCo2O4/porous graphene paper asymmetric supercapacitors with an exceptional combination of electrochemical properties. Nano Energy, 2015, 13, 306-317.	8.2	303
4	Interfacial growth of a metal–organic framework (UiO-66) on functionalized graphene oxide (GO) as a suitable seawater adsorbent for extraction of uranium( <scp>vi</scp> ). Journal of Materials Chemistry A, 2017, 5, 17933-17942.	5.2	253
5	Enhanced adsorption of uranium (VI) using a three-dimensional layered double hydroxide/graphene hybrid material. Chemical Engineering Journal, 2015, 259, 752-760.	6.6	229
6	Fabrication of ZIF-8@SiO <sub>2</sub> Micro/Nano Hierarchical Superhydrophobic Surface on AZ31 Magnesium Alloy with Impressive Corrosion Resistance and Abrasion Resistance. ACS Applied Materials & Interfaces, 2017, 9, 11106-11115.	4.0	219
7	One-step method for the fabrication of superhydrophobic surface on magnesium alloy and its corrosion protection, antifouling performance. Corrosion Science, 2014, 80, 177-183.	3.0	175
8	Removal of uranium(VI) from aqueous solutions by magnetic Schiff base: Kinetic and thermodynamic investigation. Chemical Engineering Journal, 2012, 198-199, 412-419.	6.6	161
9	Removal of uranium(VI) ions from aqueous solution by magnetic cobalt ferrite/multiwalled carbon nanotubes composites. Chemical Engineering Journal, 2015, 273, 307-315.	6.6	152
10	Fabrication of ZnO/epoxy resin superhydrophobic coating on AZ31 magnesium alloy. Chemical Engineering Journal, 2019, 368, 261-272.	6.6	150
11	Mussel-inspired functionalization of electrochemically exfoliated graphene: Based on self-polymerization of dopamine and its suppression effect on the fire hazards and smoke toxicity of thermoplastic polyurethane. Journal of Hazardous Materials, 2018, 352, 57-69.	6.5	142
12	Interconnected NiS nanosheets supported by nickel foam: Soaking fabrication and supercapacitors application. Journal of Electroanalytical Chemistry, 2015, 739, 156-163.	1.9	141
13	A graphene oxide/amidoxime hydrogel for enhanced uranium capture. Scientific Reports, 2016, 6, 19367.	1.6	128
14	Hierarchically structured layered-double-hydroxides derived by ZIF-67 for uranium recovery from simulated seawater. Journal of Hazardous Materials, 2017, 338, 167-176.	6.5	125
15	Facile synthesis of N-doped 3D graphene aerogel and its excellent performance in catalytic degradation of antibiotic contaminants in water. Carbon, 2019, 144, 781-790.	5.4	121
16	A chitosan-graphene oxide/ZIF foam with anti-biofouling ability for uranium recovery from seawater. Chemical Engineering Journal, 2020, 382, 122850.	6.6	117
17	Metallic FePSe3 nanoparticles anchored on N-doped carbon framework for All-pH hydrogen evolution reaction. Nano Energy, 2019, 57, 222-229.	8.2	115
18	Nickel-Cobalt Layered Double Hydroxide Nanowires on Three Dimensional Graphene Nickel Foam for High Performance Asymmetric Supercapacitors. Electrochimica Acta, 2016, 215, 492-499.	2.6	114

#	Article	IF	CITATIONS
19	Anchoring ZIF-67 particles on amidoximerized polyacrylonitrile fibers for radionuclide sequestration in wastewater and seawater. Journal of Hazardous Materials, 2020, 395, 122692.	6.5	104
20	Fabrication of urchin-like NiCo <sub>2</sub> (CO <sub>3</sub> ) <sub>1.5</sub> (OH) <sub>3</sub> @NiCo <sub>2</sub> S <sub>4</sub> on Ni foam by an ion-exchange route and application to asymmetrical supercapacitors. Journal of Materials Chemistry A, 2015, 3, 13308-13316.	5.2	101
21	Core-shell structure of ZnO/Co3O4 composites derived from bimetallic-organic frameworks with superior sensing performance for ethanol gas. Applied Surface Science, 2019, 475, 700-709.	3.1	101
22	Metallic and superhydrophilic nickel cobalt diselenide nanosheets electrodeposited on carbon cloth as a bifunctional electrocatalyst. Journal of Materials Chemistry A, 2018, 6, 17353-17360.	5.2	100
23	Construction of SiO2@UiO-66 core–shell microarchitectures through covalent linkage as flame retardant and smoke suppressant for epoxy resins. Composites Part B: Engineering, 2019, 176, 107261.	5.9	91
24	Porous biochar modified with polyethyleneimine (PEI) for effective enrichment of U(VI) in aqueous solution. Science of the Total Environment, 2020, 708, 134575.	3.9	89
25	Highly efficient immobilization of uranium(VI) from aqueous solution by phosphonate-functionalized dendritic fibrous nanosilica (DFNS). Journal of Hazardous Materials, 2019, 363, 248-257.	6.5	88
26	Diaminomaleonitrile functionalized double-shelled hollow MIL-101 (Cr) for selective removal of uranium from simulated seawater. Chemical Engineering Journal, 2019, 368, 951-958.	6.6	87
27	The synthesis of a manganese dioxide–iron oxide–graphene magnetic nanocomposite for enhanced uranium( <scp>vi</scp> ) removal. New Journal of Chemistry, 2015, 39, 868-876.	1.4	84
28	A novel 3D reticular anti-fouling bio-adsorbent for uranium extraction from seawater: Polyethylenimine and guanidyl functionalized hemp fibers. Chemical Engineering Journal, 2020, 382, 122555.	6.6	82
29	Ni–Mn LDH-decorated 3D Fe-inserted and N-doped carbon framework composites for efficient uranium( <scp>vi</scp> ) removal. Environmental Science: Nano, 2018, 5, 467-475.	2.2	77
30	Bovine Serum Albumin-Coated Graphene Oxide for Effective Adsorption of Uranium(VI) from Aqueous Solutions. Industrial & Engineering Chemistry Research, 2017, 56, 3588-3598.	1.8	75
31	All-solid state asymmetric supercapacitor based on NiCoAl layered double hydroxide nanopetals on robust 3D graphene and modified mesoporous carbon. Chemical Engineering Journal, 2017, 328, 873-883.	6.6	75
32	Efficient extraction of uranium from aqueous solution using an amino-functionalized magnetic titanate nanotubes. Journal of Hazardous Materials, 2018, 353, 9-17.	6.5	74
33	Graphene Oxide and Silver Ions Coassisted Zeolitic Imidazolate Framework for Antifouling and Uranium Enrichment from Seawater. ACS Sustainable Chemistry and Engineering, 2019, 7, 6185-6195.	3.2	73
34	Anti-Biofouling and Water—Stable Balanced Charged Metal Organic Framework-Based Polyelectrolyte Hydrogels for Extracting Uranium from Seawater. ACS Applied Materials & Interfaces, 2020, 12, 18012-18022.	4.0	73
35	Fabrication of super slippery sheet-layered and porous anodic aluminium oxide surfaces and its anticorrosion property. Applied Surface Science, 2015, 355, 495-501.	3.1	72
36	Synthesis, characterization and enhanced gas sensing performance of porous ZnCo <sub>2</sub> O <sub>4</sub> nano/microspheres. Nanoscale, 2015, 7, 19714-19721.	2.8	72

#	Article	IF	CITATIONS
37	High efficiency extraction of U(VI) from seawater by incorporation of polyethyleneimine, polyacrylic acid hydrogel and Luffa cylindrical fibers. Chemical Engineering Journal, 2018, 345, 526-535.	6.6	71
38	Synthesis of ZnO–Ag Hybrids and Their Gas-Sensing Performance toward Ethanol. Industrial & Engineering Chemistry Research, 2015, 54, 8947-8953.	1.8	70
39	3D self-assembly polyethyleneimine modified graphene oxide hydrogel for the extraction of uranium from aqueous solution. Applied Surface Science, 2017, 426, 1063-1074.	3.1	69
40	Recovery of uranium( <scp>vi</scp> ) from aqueous solutions using a modified honeycomb-like porous carbon material. Dalton Transactions, 2017, 46, 420-429.	1.6	68
41	Mussel-inspired anti-biofouling and robust hybrid nanocomposite hydrogel for uranium extraction from seawater. Journal of Hazardous Materials, 2020, 381, 120984.	6.5	67
42	High U(vi) adsorption capacity by mesoporous Mg(OH)2 deriving from MgO hydrolysis. RSC Advances, 2013, 3, 23278.	1.7	66
43	Novel hierarchical CoFe2Se4@CoFe2O4 and CoFe2S4@CoFe2O4 core-shell nanoboxes electrode for high-performance electrochemical energy storage. Chemical Engineering Journal, 2020, 390, 124175.	6.6	66
44	Removal U(VI) from artificial seawater using facilely and covalently grafted polyacrylonitrile fibers with lysine. Applied Surface Science, 2017, 403, 378-388.	3.1	64
45	P–p heterojunction CuO/CuCo <sub>2</sub> O <sub>4</sub> nanotubes synthesized via electrospinning technology for detecting n-propanol gas at room temperature. Inorganic Chemistry Frontiers, 2017, 4, 1219-1230.	3.0	63
46	Hyperbranched topological swollen-layer constructs of multi-active sites polyacrylonitrile (PAN) adsorbent for uranium(VI) extraction from seawater. Chemical Engineering Journal, 2019, 374, 1204-1213.	6.6	57
47	Water-repellent and corrosion-resistance properties of superhydrophobic and lubricant-infused super slippery surfaces. RSC Advances, 2017, 7, 44239-44246.	1.7	56
48	PtO 2 -nanoparticles functionalized CuO polyhedrons for n-butanol gas sensor application. Ceramics International, 2018, 44, 10426-10432.	2.3	56
49	Anti-bacterial and super-hydrophilic bamboo charcoal with amidoxime modified for efficient and selective uranium extraction from seawater. Journal of Colloid and Interface Science, 2021, 598, 455-463.	5.0	55
50	The Role of Nanobubbles in the Precipitation and Recovery of Organic-Phosphine-Containing Beneficiation Wastewater. Langmuir, 2018, 34, 6217-6224.	1.6	54
51	Nano-sized architectural design of multi-activity graphene oxide (GO) by chemical post-decoration for efficient uranium(VI) extraction. Journal of Hazardous Materials, 2019, 375, 320-329.	6.5	53
52	Mussel-inspired antifouling magnetic activated carbon for uranium recovery from simulated seawater. Journal of Colloid and Interface Science, 2019, 534, 172-182.	5.0	52
53	Defect-Induced Method for Preparing Hierarchical Porous Zr–MOF Materials for Ultrafast and Large-Scale Extraction of Uranium from Modified Artificial Seawater. Industrial & Engineering Chemistry Research, 2019, 58, 1159-1166.	1.8	52
54	Efficient removal of uranium( <scp>vi</scp> ) from simulated seawater with hyperbranched polyethylenimine (HPEI)-functionalized polyacrylonitrile fibers. New Journal of Chemistry, 2018, 42, 168-176.	1.4	51

#	Article	IF	CITATIONS
55	Insight into the performance and mechanism of low-cost phytic acid modified Zn-Al-Ti LMO for U(VI) removal. Chemical Engineering Journal, 2020, 402, 125510.	6.6	50
56	Magnetic metal-organic frameworks/carbon dots as a multifunctional platform for detection and removal of uranium. Applied Surface Science, 2019, 491, 640-649.	3.1	49
57	Designed synthesis of Ag-functionalized Ni-doped In <sub>2</sub> O <sub>3</sub> nanorods with enhanced formaldehyde gas sensing properties. Journal of Materials Chemistry C, 2019, 7, 7219-7229.	2.7	49
58	Template-free synthesis of rGO decorated hollow Co3O4 nano/microspheres for ethanol gas sensor. Ceramics International, 2018, 44, 21091-21098.	2.3	48
59	Self-assembly of graphene oxide/PEDOT:PSS nanocomposite as a novel adsorbent for uranium immobilization from wastewater. Environmental Pollution, 2019, 250, 196-205.	3.7	48
60	Enhanced acetone gas sensing response of ZnO/ZnCo2O4 nanotubes synthesized by single capillary electrospinning technology. Sensors and Actuators B: Chemical, 2017, 252, 511-522.	4.0	47
61	Hierarchical Ni–Al Layered Double Hydroxide In Situ Anchored onto Polyethylenimine-Functionalized Fibers for Efficient U(VI) Capture. ACS Sustainable Chemistry and Engineering, 2018, 6, 13385-13394.	3.2	45
62	Novel Ion-Imprinted Carbon Material Induced by Hyperaccumulation Pathway for the Selective Capture of Uranium. ACS Applied Materials & amp; Interfaces, 2018, 10, 28877-28886.	4.0	45
63	The growth and assembly of the multidimensional hierarchical Ni <sub>3</sub> S <sub>2</sub> for aqueous asymmetric supercapacitors. CrystEngComm, 2015, 17, 4495-4501.	1.3	44
64	Efficient removal of uranium( <scp>vi</scp> ) from simulated seawater using amidoximated polyacrylonitrile/FeOOH composites. Dalton Transactions, 2017, 46, 15746-15756.	1.6	44
65	Superhydrophilic phosphate and amide functionalized magnetic adsorbent: a new combination of anti-biofouling and uranium extraction from seawater. Environmental Science: Nano, 2018, 5, 2346-2356.	2.2	44
66	Efficient removal of U( <scp>vi</scp> ) from simulated seawater with hyperbranched polyethylenimine (HPEI) covalently modified SiO <sub>2</sub> coated magnetic microspheres. Inorganic Chemistry Frontiers, 2018, 5, 1321-1328.	3.0	39
67	Removal of uranium(vi) from aqueous solutions by surface modified magnetic Fe3O4 particles. New Journal of Chemistry, 2013, 37, 3914.	1.4	37
68	Simple one-step synthesis of woven amidoximated natural material bamboo strips for uranium extraction from seawater. Chemical Engineering Journal, 2021, 425, 131538.	6.6	37
69	Melamine modified graphene hydrogels for the removal of uranium( <scp>vi</scp> ) from aqueous solution. New Journal of Chemistry, 2017, 41, 10899-10907.	1.4	36
70	A novel U( <scp>vi</scp> )-imprinted graphitic carbon nitride composite for the selective and efficient removal of U( <scp>vi</scp> ) from simulated seawater. Inorganic Chemistry Frontiers, 2018, 5, 2218-2226.	3.0	36
71	Preparation and characterization of ZnO/CoNiO2 hollow nanofibers by electrospinning method with enhanced gas sensing properties. Journal of Alloys and Compounds, 2017, 702, 20-30.	2.8	35
72	Tube in tube ZnO/ZnCo <sub>2</sub> O <sub>4</sub> nanostructure synthesized by facile single capillary electrospinning with enhanced ethanol gas-sensing properties. RSC Advances, 2017, 7, 11428-11438.	1.7	35

#	Article	IF	CITATIONS
73	Facile synthesis of magnetic carboxymethylcellulose nanocarriers for pH-responsive delivery of doxorubicin. New Journal of Chemistry, 2015, 39, 7340-7347.	1.4	34
74	Synthesis of zinc-based acrylate copolymers and their marine antifouling application. RSC Advances, 2017, 7, 40020-40027.	1.7	34
75	Fabrication of electrospun Co3O4/CuO p-p heterojunctions nanotubes functionalized with HFIP for detecting chemical nerve agent under visible light irradiation. Sensors and Actuators B: Chemical, 2020, 314, 128076.	4.0	34
76	Metal-organic frameworks (MIL-68) decorated graphene oxide for highly efficient enrichment of uranium. Journal of the Taiwan Institute of Chemical Engineers, 2019, 99, 45-52.	2.7	33
77	3D hybrid Ni-Multiwall carbon nanotubes/carbon nanofibers for detecting sarin nerve agent at room temperature. Journal of Alloys and Compounds, 2019, 780, 680-689.	2.8	33
78	Preparation of magnetic core–shell iron oxide@silica@nickel-ethylene glycol microspheres for highly efficient sorption of uranium(vi). Dalton Transactions, 2015, 44, 6909-6917.	1.6	32
79	Polypyrrole/cobalt ferrite/multiwalled carbon nanotubes as an adsorbent for removing uranium ions from aqueous solutions. Dalton Transactions, 2016, 45, 9166-9173.	1.6	31
80	Investigation of uranium (VI) adsorption by poly(dopamine) functionalized waste paper derived carbon. Journal of the Taiwan Institute of Chemical Engineers, 2018, 91, 266-273.	2.7	31
81	Monodisperse and core–shell structured NaYF4:Ln@SiO2 (Ln=Yb/Er, Yb/Tm) microspheres: Synthesis and characterization. Journal of Alloys and Compounds, 2010, 490, 684-689.	2.8	30
82	Designed synthesis of Co-doped sponge-like In <sub>2</sub> O <sub>3</sub> for highly sensitive detection of acetone gas. CrystEngComm, 2019, 21, 1876-1885.	1.3	30
83	Three-dimensional hierarchical Co <sub>3</sub> O <sub>4</sub> nano/micro-architecture: synthesis and ethanol sensing properties. CrystEngComm, 2016, 18, 5728-5735.	1.3	29
84	Heterogeneous NiSe <sub>2</sub> /Ni Ultrafine Nanoparticles Embedded into an N,S-Codoped Carbon Framework for pH-Universal Hydrogen Evolution Reaction. ACS Sustainable Chemistry and Engineering, 2019, 7, 4119-4127.	3.2	29
85	Electrospun n-p WO3/CuO heterostructure nanofibers as an efficient sarin nerve agent sensing material at room temperature. Journal of Alloys and Compounds, 2019, 793, 31-41.	2.8	27
86	An anti-algae adsorbent for uranium extraction: l-Arginine functionalized graphene hydrogel loaded with Ag nanoparticles. Journal of Colloid and Interface Science, 2019, 543, 192-200.	5.0	27
87	3D hierarchical CoFe2O4/CoOOH nanowire arrays on Ni-Sponge for high-performance flexible supercapacitors. Electrochimica Acta, 2020, 340, 135892.	2.6	27
88	Bioinspired Reduced Graphene Oxide/Polyacrylonitrileâ€Based Carbon Fibers/CoFe <sub>2</sub> O <sub>4</sub> Nanocomposite for Flexible Supercapacitors with High Strength and Capacitance. ChemElectroChem, 2018, 5, 1297-1305.	1.7	26
89	Fast self-replenishing slippery surfaces with a 3D fibrous porous network for the healing of surface properties. Journal of Materials Chemistry A, 2019, 7, 24900-24907.	5.2	26
90	Preparation of magnetic calcium silicate hydrate for the efficient removal of uranium from aqueous systems. RSC Advances, 2015, 5, 5904-5912.	1.7	25

#	Article	IF	CITATIONS
91	Porous tungsten trioxide nanolamellae with uniform structures for high-performance ethanol sensing. CrystEngComm, 2016, 18, 8411-8418.	1.3	25
92	Fabrication of CeO <sub>2</sub> /ZnCo <sub>2</sub> O <sub>4</sub> n–p heterostructured porous nanotubes via electrospinning technology for enhanced ethanol gas sensing performance. RSC Advances, 2016, 6, 101626-101637.	1.7	24
93	Swollen-layer constructed with polyamine on the surface of nano-polyacrylonitrile cloth used for extract uranium from seawater. Chemosphere, 2021, 271, 129548.	4.2	24
94	High efficiency biosorption of Uranium (VI) ions from solution by using hemp fibers functionalized with imidazole-4,5-dicarboxylic. Journal of Molecular Liquids, 2020, 297, 111739.	2.3	23
95	HFIP-functionalized electrospun WO3 hollow nanofibers/rGO as an efficient double layer sensing material for dimethyl methylphosphonate gas under UV-Light irradiation. Journal of Alloys and Compounds, 2020, 832, 154999.	2.8	23
96	Preparation of a 3D multi-branched chelate adsorbent for high selective adsorption of uranium(VI): Acrylic and diaminomaleonitrile functionalized waste hemp fiber. Reactive and Functional Polymers, 2020, 149, 104512.	2.0	22
97	Synthesis of hybrid zinc/silyl acrylate copolymers and their surface properties in the microfouling stage. RSC Advances, 2016, 6, 13858-13866.	1.7	21
98	Hierarchical flower like double-layer superhydrophobic films fabricated on AZ31 for corrosion protection and self-cleaning. New Journal of Chemistry, 2017, 41, 12767-12776.	1.4	21
99	HFIPâ€Functionalized Co <sub>3</sub> O <sub>4</sub> Microâ€Nanoâ€Octahedra/rGO as a Doubleâ€Layer Sensing Material for Chemical Warfare Agents. Chemistry - A European Journal, 2019, 25, 11892-11902.	1.7	21
100	Preparation of NiAl-LDH/Polypyrrole composites for uranium(VI) extraction from simulated seawater. Colloids and Surfaces A: Physicochemical and Engineering Aspects, 2019, 562, 329-335.	2.3	21
101	Polypyrrole modified Fe <sup>0</sup> -loaded graphene oxide for the enrichment of uranium( <scp>vi</scp> ) from simulated seawater. Dalton Transactions, 2018, 47, 12984-12992.	1.6	20
102	Comprehensive biocompatible hemp fibers improved by phosphate zwitterion with high U(VI) affinity in the marine conditions. Chemical Engineering Journal, 2022, 430, 132742.	6.6	19
103	Phosphatidyl-assisted fabrication of graphene oxide nanosheets with multiple active sites for uranium(vi) capture. Environmental Science: Nano, 2018, 5, 1584-1594.	2.2	18
104	Hierarchical structure of CoFe2O4 core-shell microsphere coating on carbon fiber cloth for high-performance asymmetric flexible supercapacitor applications. Ionics, 2019, 25, 4905-4914.	1.2	18
105	Solvent ratio controlled synthesis of CoFe2O4 hollow skeleton nanobox electrode for high-performance supercapacitor. Applied Surface Science, 2020, 533, 147433.	3.1	18
106	A hybrid sponge with guanidine and phytic acid enriched surface for integration of antibiofouling and uranium uptake from seawater. Applied Surface Science, 2020, 525, 146611.	3.1	18
107	Composites of hierarchical metal–organic framework derived nitrogen-doped porous carbon and interpenetrating 3D hollow carbon spheres from lotus pollen for high-performance supercapacitors. New Journal of Chemistry, 2017, 41, 12835-12842.	1.4	17
108	Improvement of U(VI) removal by tuning magnetic metal organic frameworks with amine ligands. Journal of Molecular Liquids, 2021, 334, 116495.	2.3	17

XIN WANG

#	Article	IF	CITATIONS
109	Longâ€Term Stability of a Liquidâ€Infused Coating with Antiâ€Corrosion and Antiâ€Icing Potentials on Al Alloy. ChemElectroChem, 2019, 6, 3911-3919.	1.7	16
110	The study of metallic uranium production by pyrochemical mix-conversion of U3O8. Electrochimica Acta, 2019, 318, 194-201.	2.6	15
111	Grown Carbon Nanotubes on Electrospun Carbon Nanofibers as a 3D Carbon Nanomaterial for High Energy Storage Performance. ChemistrySelect, 2019, 4, 5437-5458.	0.7	15
112	Synthesis of Amphiphilic Acrylate Boron Fluorinated Polymers with Antifouling Behavior. Industrial & Engineering Chemistry Research, 2019, 58, 8016-8025.	1.8	15
113	Ionic liquid combined with NiCo2O4/rGO enhances electrochemical oxygen sensing. Talanta, 2020, 209, 120515.	2.9	15
114	The structures of CoFe2O4/PEDOT electrodes effect on the stability and specific capacity for electrochemical energy storage. Applied Surface Science, 2021, 542, 148670.	3.1	15
115	In situ construction of 3-dimensional hierarchical carbon nanostructure; investigation of the synthesis parameters and hydrogen evolution reaction performance. Carbon, 2021, 178, 48-57.	5.4	14
116	Synthesis of C@Ni-Al LDH HSS for efficient U-entrapment from seawater. Scientific Reports, 2019, 9, 5807.	1.6	13
117	The efficient immobilization of uranium( <scp>vi</scp> ) by modified dendritic fibrous nanosilica (DFNS) using mussel bioglue. Inorganic Chemistry Frontiers, 2019, 6, 746-755.	3.0	12
118	Ion cross-linking assisted synthesis of ZIF-8/chitosan/melamine sponge with anti-biofouling activity for enhanced uranium recovery. Inorganic Chemistry Frontiers, 2021, 9, 155-164.	3.0	12
119	Mussel-inspired polydopamine microspheres self-adhered on natural hemp fibers for marine uranium harvesting and photothermal-enhanced antifouling properties. Journal of Colloid and Interface Science, 2022, 622, 109-116.	5.0	12
120	In Situ Anchoring of Pyrrhotite on Graphitic Carbon Nitride Nanosheet for Efficient Immobilization of Uranium. Chemistry - A European Journal, 2019, 25, 590-597.	1.7	11
121	Bifunctional Conducting Polymer Coated CoFe 2 O 4 Core‧hell Nanolayer on Carbon Fiber Cloth for 2.0â€V Wearable Aqueous Supercapacitors. ChemistrySelect, 2019, 4, 1685-1695.	0.7	11
122	Facile Construction of Sandwichâ€like Co <sub>3</sub> O <sub>4</sub> /CNTs Complex for Highâ€performance Asymmetric Supercapacitors. ChemistrySelect, 2019, 4, 3878-3883.	0.7	10
123	Synthesis of microporous aromatic framework with scholl-coupling reaction for efficient uranium (VI) capture. Colloids and Surfaces A: Physicochemical and Engineering Aspects, 2020, 602, 125131.	2.3	10
124	Inâ€situ Immobilization of a Polyoxometalate <scp>Metalâ€Organic</scp> Framework ( <scp>NENU</scp> â€3) on Functionalized Reduced Graphene Oxide for Hydrazine Sensing. Chinese Journal of Chemistry, 2021, 39, 2889-2897.	2.6	10
125	Atomically dispersed Ni–N4 species and Ni nanoparticles constructing N-doped porous carbon fibers for accelerating hydrogen evolution. Carbon, 2021, 185, 96-104.	5.4	10
126	Co-construction of molecular-level uranyl-specific "nano-holes―with amidoxime and amino groups on natural bamboo strips for specifically capturing uranium from seawater. Journal of Hazardous Materials, 2022, 437, 129407.	6.5	10

#	Article	IF	CITATIONS
127	Uranium(vi) adsorption on alumina hollow microspheres synthesized via a facile self-templating process. RSC Advances, 2013, 3, 6621.	1.7	9
128	Combination therapeutics of doxorubicin with Fe <sub>3</sub> O <sub>4</sub> @chitosan@phytic acid nanoparticles for multi-responsive drug delivery. RSC Advances, 2016, 6, 88248-88254.	1.7	8
129	Effect of the synthesis method on the performance of Fe3O4–inositol hexaphosphate as a drug delivery vehicle for combination therapeutics with doxorubicin. New Journal of Chemistry, 2017, 41, 5305-5312.	1.4	8
130	Electrochemical study of reduction Ce(III) ions and production of high purity metallic cerium by electrorefining in fused LiCl-KCl eutectic. Journal of Electroanalytical Chemistry, 2020, 878, 114691.	1.9	8
131	Water-locking molecule-assisted fabrication of nature-inspired Mg(OH) <sub>2</sub> for highly efficient and economical uranium capture. Dalton Transactions, 2020, 49, 7535-7545.	1.6	8
132	MOF-derived electrochemical catalyst Cu–N/C for the enhancement of amperometric oxygen detection. Nanoscale, 2022, 14, 1796-1806.	2.8	8
133	Electrochemical Mixâ€Reduction Process of U and Uâ€Fe Alloys on the Surface of Cathode in LiClâ€KClâ€U <sub>3</sub> O <sub>8</sub> at 773â€K. ChemElectroChem, 2018, 5, 2738-2746.	1.7	7
134	Fully Repairable Slippery Organogel Surfaces with Reconfigurable Paraffin-Based Framework for Universal Antiadhesion. ACS Applied Materials & Interfaces, 2020, 12, 39807-39816.	4.0	7
135	HFIP-functionalized 3D carbon nanostructure as chemiresistive nerve agents sensors under visible light. Sensors and Actuators B: Chemical, 2022, 358, 131475.	4.0	7
136	Surface morphology properties and antifouling activity of Bi2WO6/boron-grafted polyurethane composite coatings realized via multiple synergy. Journal of Colloid and Interface Science, 2022, 626, 815-823.	5.0	7
137	Photocatalytic antifouling coating based on carbon nitride with dynamic acrylate boron fluorinated polymers. New Journal of Chemistry, 2021, 45, 780-787.	1.4	5
138	Ag-CS Enhanced Performance of Pyrrolidone-Based Ionic Liquid Oxygen Sensor. Journal of the Electrochemical Society, 2020, 167, 067522.	1.3	3
139	αâ^'Fe2O3/rGO cooperated with tri-alkyl-substituted-imidazolium ionic liquids for enhancing oxygen sensing. Sensors and Actuators B: Chemical, 2021, 341, 130029.	4.0	3
140	Theory-Guided Design of a Method to Obtain Competitive Balance between U(VI) Adsorption and Swaying Zwitterion-Induced Fouling Resistance on Natural Hemp Fibers. International Journal of Molecular Sciences, 2022, 23, 6517.	1.8	3
141	Electrochemical Mix-Reduction Process of U and U-Fe Alloys on the Surface of Cathode in LiCl-KCl-U3 O8 at 773â€K. ChemElectroChem, 2018, 5, 2697-2697.	1.7	1
142	Constructing three-dimensional network C, O Co-doped nitrogen-deficient carbon nitride regulated by acrylic fluoroboron overall marine antifouling. Journal of Colloid and Interface Science, 2022, 608, 1802-1812.	5.0	1
143	Design of multifunctional phytate coated magnetic composites for combined therapy with antitumor drugs. New Journal of Chemistry, 2017, 41, 14898-14905.	1.4	0